



ELSEVIER

Available online at www.sciencedirect.com

ScienceDirect

Proceedings of the Combustion Institute 000 (2018) 1–11

Proceedings
of the
Combustion
Institutewww.elsevier.com/locate/proci

Study of mechanisms for electric field effects on ethanol oxidation via reactive force field molecular dynamics

Xi Zhuo Jiang, Muye Feng, Weilin Zeng, Kai H. Luo*

*Department of Mechanical Engineering, University College London, Torrington Place, London WC1E 7JE, United Kingdom*Received 27 November 2017; accepted 10 July 2018
Available online xxx

Abstract

Molecular dynamics simulations based on reactive force fields (ReaxFF) were conducted to study the effects of an external electric field with varying electric field strengths on ethanol oxidation reactions. Time evolutions of the reactants and intermediate species indicate that imposition of the electric field has modified the reaction pathways in addition to changing the reaction rate in a non-linear way. Intermediates of ethanol oxidation reactions with and without the electric field are identified and quantified. For the first time, reaction pathways of ethanol oxidation with and without an imposed electric field are scrutinized at the atomic scales. The reaction pathways without the electric field are consistent with previous experimental and numerical studies, which validate the present approach. Reaction pathways under varying electric field strengths, on the other hand, show some common pathways but also unique pathways associated with different strengths of the imposed electric field. The ReaxFF-based molecular dynamics method provides new insight into mechanisms for the effects of an electric field with varying electric field strengths on ethanol oxidation reactions. The present research demonstrates that ReaxFF-based reactive molecular dynamics is a valuable tool for detailed study of reaction mechanisms of hydrocarbon or oxygenated fuels, which complements commonly used experimental and computational techniques.

© 2018 The Author(s). Published by Elsevier Inc. on behalf of The Combustion Institute.

This is an open access article under the CC BY license. (<http://creativecommons.org/licenses/by/4.0/>)*Keywords:* Ethanol oxidation; Electric field; Reactive force field molecular dynamics; Reaction pathways

1. Introduction

The effects of an electric field on combustion have long been recognized and reported [1]. The electric field can deform the flame shape [2], alter

flame instabilities [3–5] and reduce pollutant emissions [6]. Due to their impact on flame behaviors, the electric field has been applied to many fields, such as modifying the flame quenching performance [7], affecting mass spectrometric sampling of ions from a flame [8], and synthesizing nanostructures like Titania [9] and carbon nanotubes [10]. Ethanol, as a biomass-derived fuel, can contribute to reducing reliance on traditional fossil

* Corresponding author.

E-mail address: K.Luo@ucl.ac.uk (K.H. Luo).<https://doi.org/10.1016/j.proci.2018.07.053>1540-7489 © 2018 The Author(s). Published by Elsevier Inc. on behalf of The Combustion Institute. This is an open access article under the CC BY license. (<http://creativecommons.org/licenses/by/4.0/>)

Please cite this article as: X.Z. Jiang et al., Study of mechanisms for electric field effects on ethanol oxidation via reactive force field molecular dynamics, Proceedings of the Combustion Institute (2018), <https://doi.org/10.1016/j.proci.2018.07.053>

fuels [11,12]. Ethanol oxidation reactions under special circumstances, such as in hydrothermal oxidation [13], in combustion [14], and behind the shock waves [15], have been widely studied. By a simple extension, one would expect that the oxidation reactions of ethanol can be controllable if an electric field is applied.

Previous studies on ethanol oxidation shed light on distinguished phenomena in the presence of an electric field. For example, Luo et al. [16] revealed that the velocity fields, mass fraction distributions and temperature fields in a small diffusion flame are modified by the electric field. Imamura et al. reported flame deformation of ethanol droplets in different vertical electric field strengths experimentally [2] and investigated the relation between the applied voltage and electrode distance in their follow-on studies [17]. These findings contribute to our understanding of flame behaviors under the electric field. However, some fundamental questions remain unsolved. For instance, what changes in physicochemical quantities are behind the observed phenomena in the presence of an electric field? Would the electric field strength affect the reaction rates monotonously or nonlinearly? Would the electric field modify the reaction pathways? Due to their inherent limitations, conventional experiments and continuum numerical simulations have not answered in-depth questions like these, which are related to the interactions between the electrical field and the flame behaviors at the atomic scales.

To resolve these issues, studies focusing on the atomic events of ethanol oxidation are required. Molecular dynamics (MD) provides a possibility to uncover the atomic events behind the reaction kinetics. However, classical MD force fields are unable to describe bond breaking, bond formation or chemical reactivity. Quantum mechanics methods can provide accurate reaction information for individual elementary reactions, but are computationally too expensive to deal with a realistic reactive system. An attractive alternative method is the reactive force field (ReaxFF) MD method [18–20], which can describe complex chemical reactions at affordable computational cost [21,22].

ReaxFF employs a bond-order formalism in conjunction with polarizable charge descriptions to describe both reactive and non-reactive interactions between atoms. This allows ReaxFF to accurately model both covalent and electrostatic interactions for a diverse range of materials. The potential energy of a system can be calculated by Eq. (1).

$$E_{\text{system}} = E_{\text{bond}} + E_{\text{over}} + E_{\text{under}} + E_{\text{lp}} + E_{\text{val}} + E_{\text{tors}} + E_{\text{Coulomb}} + E_{\text{vdW}} \quad (1)$$

In Eq. (1), the first six terms on the right-hand side are bonding terms. E_{bond} describes the en-

ergy associated with forming bonds between atoms and is a function of the interatomic distance. E_{over} and E_{under} are an energy penalty preventing the over- and under-coordination of atoms based on atomic valence rules, respectively. E_{lp} is the long pair energy. E_{val} and E_{tors} are the energies associated with three-body valence angle strain and four-body torsional angle strain, respectively. E_{Coulomb} and E_{vdW} are non-bond terms, representing electrostatic and dispersive contributions calculated between all atoms, regardless of connectivity and bond-order [23]. Further information about the ReaxFF formation and development can be found in previous studies [19,20,24]. ReaxFF-based MD has found applications in diverse fields including catalytic combustion [25], soot formation [26,27] and fuel evaporation [28].

In this research, MD simulations based on ReaxFF are conducted to investigate the effects of an external electric field with varying electric field strengths on ethanol oxidation reactions. Time evolutions of the two reactants are investigated first, followed by identification of intermediate species. To further reveal the effects of the electric field on the ethanol oxidation reactions, reaction pathways with and without an electric field are explored. The reaction pathways reveal different radical behaviors with and without the electric field.

2. Computational methods

2.1. Case set-ups

To study the effects of the electric field on oxidation of ethanol, three electric strength values based on previous experimental and computational studies [2,16,17] (i.e., 10^{-6} V/Å, 10^{-5} V/Å, and 10^{-4} V/Å) are applied to the system. For comparisons, an oxidation system without any external electric field is also studied. The reacting case without an imposed electric field is thereafter called the base case. Three replicas individually with different initial configurations are established for every scenario. Therefore, twelve MD simulations have been conducted and analyzed.

Every system is heated from 300 K to 3000 K at the initial stage of 500 ps, and during this period no electric field is imposed upon the system. After the initial 500 ps, the temperature of the system is maintained at 3000 K, and the electric field with the aforementioned strength is imposed only in the +x direction.

2.2. Simulation details

MD simulations based on the C/H/O ReaxFF force field are performed using the canonical (NVT) ensemble under the Nosé–Hoover thermostat algorithm with a damping constant of

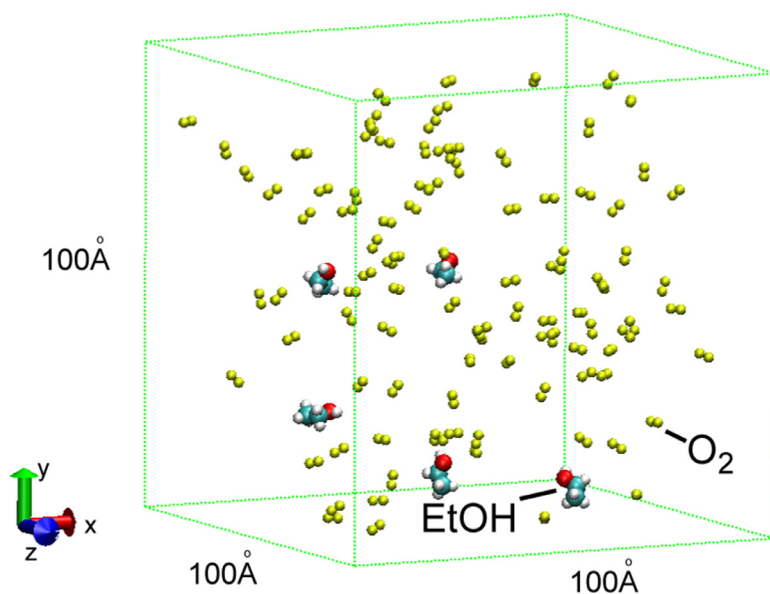


Fig. 1. A representative initial configuration for ethanol oxidation.

100 fs. The newly developed CHO-2016 parameter set [23], which has improved performance in C_1 chemistry compared to its popular 2008 counterpart [19], is selected for the oxidation of ethanol molecules. The dimension of each simulation box is $100 \times 100 \times 100 \text{ \AA}^3$. Five ethanol (EtOH) and 100 oxygen (O_2) molecules are included in every simulation system. The periodic boundary conditions are implemented in all three directions. Before “production” simulations, every system is energy minimized for 40 ps at 300 K to eliminate simulation artifacts that could cause simulation collapses. A typical initial configuration (from one replica) for the oxidation system is shown in Fig. 1.

A time step of 0.1 fs is found to be appropriate and the dynamic trajectories are recorded every 1 ps. All the simulations are carried out with the REAXC package in the LAMMPS platform [29]. For most of the simulations, the total physical times are determined by the total consumption of EtOH molecules.

A 0.3 bond order cutoff [30] for molecular recognition is selected to analyze the intermediates and products formed during the reactive MD simulations.

All the parallel MD simulations are carried out on ARCHER, the UK national supercomputing service. Post-processing of the MD results is accomplished using self-developed PYTHON (Python Software Foundation, Wilmington, De) scripts. The reaction pathways are summarised using the ChemTraYzer scripts [31]. The visualization of molecular structures is performed by VMD [32] package.

3. Results and discussion

3.1. Validation of the method

To validate the ReaxFF MD method, ethanol pyrolysis simulations are conducted and the intermediates of pyrolysis reactions from the ReaxFF MD simulation are compared with those from the experiments. In the initial stage of the pyrolysis, CH_2 , CH_2O , CH_3 , CH_4 , CH_3O , CH_4 , CH_4O , C_2H_4 , C_2H_4O , C_2H_5 , CO , H_2 and H_2O are observed in the MD simulation. The occurrence of these species is also reported in previous experimental studies [33,34], which suggests the validity of the ReaxFF MD method.

The effects of the electric field on oxidation reactions are discussed in the following sections. Common initial configurations are used among simulation cases with and without the electric field and the statistics are averaged among replicas in every situation.

3.2. Effects of electric field on EtOH oxidation reactions

3.2.1. Time evolution of reactants

The numbers of the reactants (i.e., EtOH and O_2 molecules) are recorded as shown in Fig. 2. The constants for first order reactions (Eq. (2)) of both EtOH and O_2 molecules are calculated for different stages of the reactions as listed in Table 1.

$$\frac{-d[A]}{dt} = k[A] \quad (2)$$

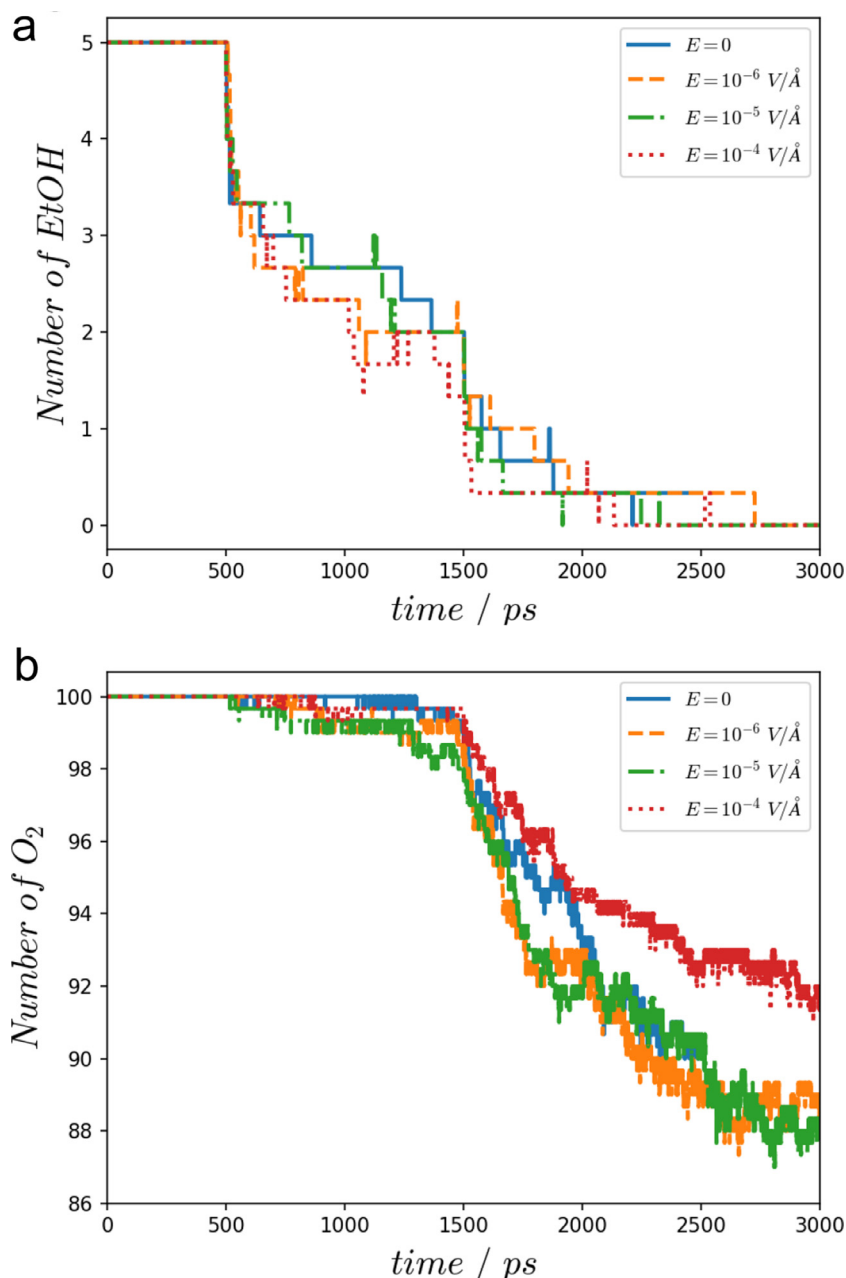


Fig. 2. Time evolution of (a) EtOH molecule number and (b) O_2 molecular number.

where $[A]$ is the concentration of the reactants, and k is the constant for the reactant of interest with the unit of s^{-1} .

During the first 1500 ps, the electric field generally promotes the consumption of EtOH molecules (Fig. 2(a)) with the reaction rate constant k increasing with the electric field strength. Thereafter, how-

ever, the electric field influence is more complicated. As for O_2 molecules shown in Fig. 2(b), during the first 1500 ps, the electric field tends to accelerate the consumption of O_2 molecules as the coefficients in those cases with an electric field are greater than that in the base case. After that, reversed effects of the electric field are observed: the reaction of O_2 is

Table 1

Constants of first order reactions, k , of EtOH and O₂ at different stages ($\times 10^7$ s⁻¹).

$E/V \text{ \AA}^{-1}$	EtOH		O ₂	
	500–1500 ps		500–1500 ps	1500–2000 ps
0	1.450 ± 0.006		0.413 ± 0.005	8.336 ± 0.018
10 ⁻⁶	1.548 ± 0.010		1.162 ± 0.007	7.805 ± 0.026
10 ⁻⁵	1.840 ± 0.006		1.303 ± 0.006	6.395 ± 0.030
10 ⁻⁴	1.988 ± 0.010		0.468 ± 0.003	5.912 ± 0.015

decelerated in the presence of the electric field, and the deceleration is aggravated as the electric field strength increases.

Figure 2 witnesses the modification of reaction rates of the two reactants in the ethanol oxidation reactions by the electric field, but whether the electric field causes the generation of new species or merely changes the reaction rates without altering the intermediate species varieties is still unknown. To check whether new species are formed, the intermediates in reactions with and without the electric field are scrutinized.

3.2.2. Intermediates

The number of species at each instant is monitored as shown in Fig. 3(a), and discrepancy in the time evolution trends of species numbers can be observed as expected. For the base case and the median electric field ($E = 10^{-5}$ V/Å) case, the number of species reaches its peak promptly after the reaction begins and remains almost unchanged till the end of the reaction. As for the weak ($E = 10^{-6}$ V/Å) and strong ($E = 10^{-4}$ V/Å) electric field cases, the number of species first ascends to a median value and then gradually climbs to the maximum.

Furthermore, the varieties of intermediate species are compared among cases with and without the electric field. Common intermediates among these cases and unique intermediates in each situation are also identified. As shown in Fig. 3(b), CH₂O, CH₃, CH₃O, CH₃O₂, CH₃O₃, C₂H₄, C₂H₅, C₂H₅O, C₂H₅O₂, H, HO, HO₂, H₂O and O are broadly shared among the four cases. H₂ molecules are observed only in the base case and the strong electric field case, and CH₂ are produced in the weak and median electric field cases. CH₂O₂ is exclusively found in the $E = 10^{-5}$ V/Å case.

Time evolutions of the numbers of four representative intermediates (i.e., CH₃O, C₂H₅, HO, and O) under the varying electric field strengths are also investigated as shown in Fig. 4. Though the numbers of CH₃O and C₂H₅ are minuscule due to the limited number of the input ethanol molecules (only five ethanol molecules at the very beginning), differences in the trend of individual species quantity can still be recognized. For example, the electric field of 10⁻⁶ V/Å favors the formation of CH₃O from 500 to 1500 ps (Fig. 4(a)), while C₂H₅ rad-

icals experience rapid generation as well as fast consumption under the electric field of 10⁻⁴ V/Å (Fig. 4(b)).

HO and O radicals are gradually generated from 500 to 1500 ps as reactions of ethanol and oxygen proceed, but the following period (after 1500 ps) witnesses explosive increases in both radicals. Throughout the whole process, the effects of the electric field exhibit non-linear behaviors. For instance, in Fig. 4(c), the electric field with the strong strength (10⁻⁴ V/Å) promotes the generation of HO radicals from 500 to 1500 ps, and the number of HO radicals overwhelms its $E = 0$ counterpart in this period. However, after 1500 ps, the number of HO radicals in the $E = 10^{-4}$ V/Å case is quickly surpassed by its $E = 0$ counterpart.

The above findings regarding the different types of intermediate species and the discrepancies in their time evolutions demonstrate that imposition of an electric field on the ethanol oxidation reaction modifies the reaction pathways, rather than merely changes the reaction rate with reaction pathways intact.

3.3. Discussion – reaction pathways and intermediates

Imposing an electric field may affect the reaction pathways through several mechanisms. The direct action of the imposed electric field is on charged particles (cations, anions, and electrons), which moves them away from the reaction zone where ion-electron recombination usually takes place to reduce the number of charged particles. As a result, fuel chemistry is modified. In the meantime, the charged particles can be accelerated by the electric field. The kinetic energy gained from the acceleration could influence reaction rates associated with charged particles. The accelerated charged particles also transfer momentum to neutral molecules by collision, which results in the generation of bulk flow in the form of an ionic wind. Acceleration and collision of charged and neutral particles could enhance diffusion flux, thereby modifying the reaction rates.

To identify the effects of an external electric field on the reaction mechanisms, the reaction pathways for ethanol oxidation at the initial stage

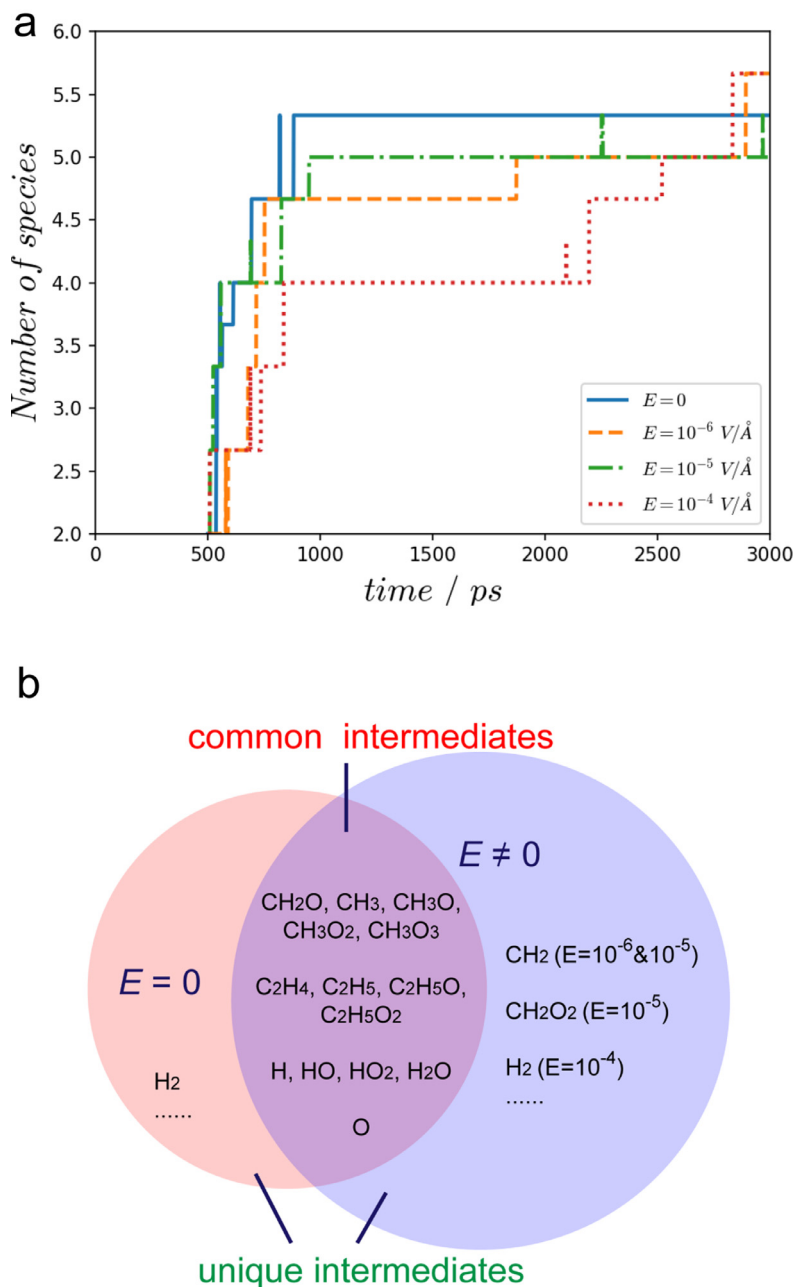


Fig. 3. (a) Time evolution of species number and (b) common intermediates and unique intermediates among cases with and without an electric field.

(from 500 to 1500 ps) are examined via the widely used the ChemTraYzer scripts [31]. Reaction pathways studied are summarized and compared in Table 2.

Four elementary reactions are observed at the very beginning among all the four cases, and these four elementary reactions depict the ba-

sic steps of the reaction between EtOH and O_2 : the pyrolysis of ethanol molecules occurs (Pathways R1–R3 in Table 2) before oxygen molecules oxidize the radicals stemming from the pyrolysis of ethanol molecules (Pathway R4 in Table 2). These steps were also reported in an experimental study on high-energy combustion systems of

Table 2

Reaction pathways at the initial stage of ethanol oxidation reactions. The solid circle means the corresponding reaction pathway is detected in the referred situation.

No.	Reaction Pathways	E/V·Å ⁻¹			
		0	10 ⁻⁶	10 ⁻⁵	10 ⁻⁴
Common pathways					
R1	C ₂ H ₆ O ↔ C ₂ H ₅ + HO	•	•	•	•
R2	C ₂ H ₆ O ↔ CH ₃ O + CH ₃	•	•	•	•
R3	C ₂ H ₅ ↔ C ₂ H ₄ + H	•	•	•	•
R4	O ₂ + H ↔ HO + O	•	•	•	•
R5	C ₂ H ₆ O ↔ C ₂ H ₅ O + H	•	•	•	
R6	C ₂ H ₆ O + H ↔ C ₂ H ₅ + H ₂ O	•		•	•
R7	HO ₂ ↔ HO + O	•	•		
R8	O ₂ + H ↔ HO ₂	•	•		
R9	C ₂ H ₅ O ↔ C ₂ H ₄ + HO	•		•	
Unique pathways					
R10	C ₂ H ₆ O + H ↔ C ₂ H ₅ O + H ₂	•			
R11	C ₂ H ₄ + O ↔ CH ₂ O + CH ₂		•		
R12	C ₂ H ₅ O ↔ CH ₂ O + CH ₃		•		
R13	C ₂ H ₆ O + HO ↔ C ₂ H ₅ O + H ₂ O		•		
R14	O ₂ ↔ O + O		•		
R15	C ₂ H ₆ O + O ↔ C ₂ H ₅ O + HO			•	
R16	CH ₂ O + HO ↔ CH ₂ O ₂ + H			•	
R17	CH ₃ O + H ↔ CH ₄ O			•	
R18	CH ₄ O ↔ CH ₃ + HO			•	
R19	HO ₂ ↔ O ₂ + H			•	
R20	HO + O ↔ HO ₂			•	
R21	O ₂ + CH ₂ ↔ CH ₂ O ₂			•	
R22	O ₂ + CH ₃ ↔ HO ₂ + CH ₂			•	
R23	C ₂ H ₅ + H ↔ C ₂ H ₄ + H ₂				•
R24	H ₂ O + H ↔ H ₂ + HO				•

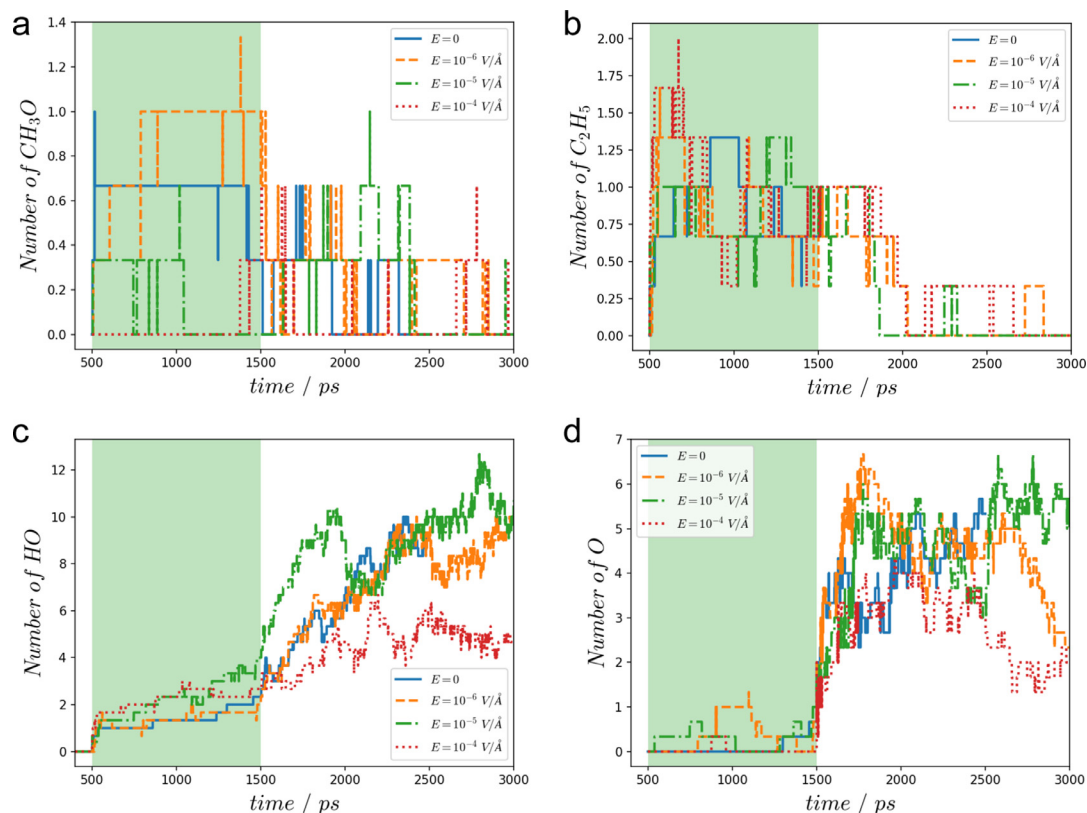


Fig. 4. Time evolutions of common radical numbers. (a) CH_3O , (b) C_2H_5 , (c) HO , and (d) O . The effects of the electric field on the time evolutions of the radicals are non-linear, which indicates alteration of the reaction pathways by the imposed electric field.

EtOH , like shock-induced ignition of ethanol-air mixtures [35]. For the four common elementary reactions, the proportions of the occurrence time of each elementary reaction to the aggregate occurrence time of all the reactions in each simulation case are shown in Fig. 5(a). It is clear that the significance of each elementary reaction in the ethanol oxidation reaction differs as the electric field varies. Furthermore, an element flux analysis [36,37] was also conducted to estimate the significance of the two reactions involving $\text{C}_2\text{H}_6\text{O}$ (i.e., R1 and R2), and the results suggest that R1 plays a more significant role than R2 in all the four simulations regardless of whether the electric field is imposed or not. (Detailed estimation can be found in the supplementary material.)

Figure 4(b) illustrates a large quantity of C_2H_5 radicals in the $E=10^{-4} \text{ V/Å}$ case, which can be attributed to the high percentage of the reaction $\text{C}_2\text{H}_6\text{O} \leftrightarrow \text{C}_2\text{H}_5 + \text{HO}$ (R1) under the electric field with the strength of 10^{-4} V/Å (in Fig. 5(a)). Analogously, the high percentage of R2 in the presence of the electric field of 10^{-6} V/Å contributes to the high level of CH_3O in quantity as illustrated in

Fig. 4(a). In R3, the generation of the radical H provides one reactant of R4, and the high percentage of R3 in the $E=10^{-4} \text{ V/Å}$ case benefits the forward reaction of R4, thereby promoting the formation of OH radicals at the initial stage.

Meanwhile, the instants of the first occurrence of the O radical in the four cases are recorded as well. As shown in Fig. 5(b), the $E=10^{-4} \text{ V/Å}$ case has the earliest occurrence of the O radical with the base case having the latest appearance of the O radical. This order, in the meantime, explains the differences in the consumption rate of O_2 from 500 to 1500 ps (Fig. 2(b)), since O radicals at the very initial stage mainly stem from the elementary reaction $\text{O}_2 + \text{H} \leftrightarrow \text{HO} + \text{O}$ (R4) where O_2 molecules are consumed.

Furthermore, the unique pathways associated with different strengths of the electric field listed in Table 2 further elucidate the intricate effects of the electric field on ethanol oxidation mechanisms, which are also illustrated in Fig. 3(b). H_2 molecules are common intermediates for the base case and the $E=10^{-4} \text{ V/Å}$ case. However, H_2 molecules of the base case are produced by the elementary

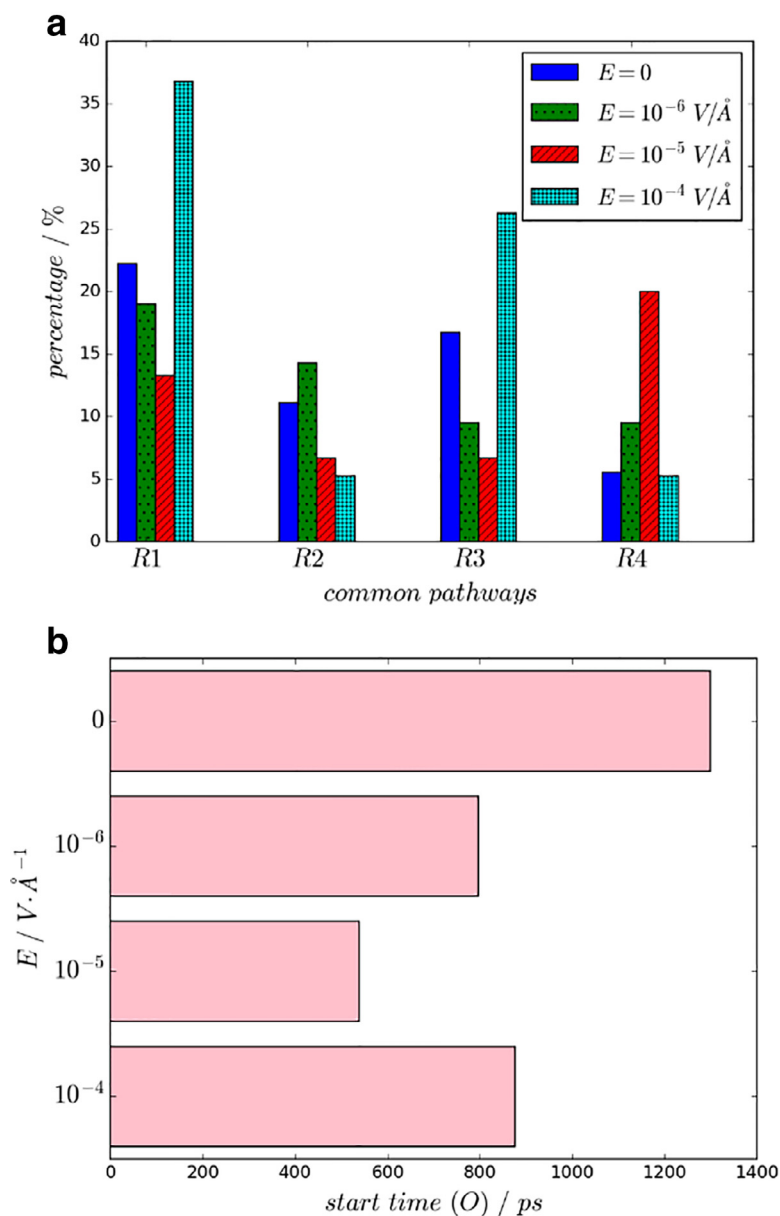


Fig. 5. (a) The percentages of the four common elementary reactions in Table 2, and (b) time instant of the first occurrence of the O radical in each simulation case.

reaction R10, with its $E = 10^{-4} \text{ V/\AA}$ counterpart from reaction R23. Similarly, CH_2 radicals are shared between $E = 10^{-6} \text{ V/\AA}$ and $E = 10^{-5} \text{ V/\AA}$ cases, but the radicals stem from reactions R11 and R22, respectively. The unique intermediate CH_2O_2 radicals detected in the $E = 10^{-5} \text{ V/\AA}$ case are products of the exclusive reactions R16 and R21 found under this electric field strength.

4. Conclusions

In this research, molecular dynamics simulations based on ReaxFF were conducted to investigate the effects of an external electric field with varying electric field strengths on ethanol oxidation reactions. Time evolutions of the reactants and intermediate species indicate that imposition of the electric field has modified the reaction pathways in

addition to changing the reaction rates of individual elementary reactions. Three cases with varying strengths of the electric field are simulated with the ReaxFF MD, together with a case without the electric field imposed. Common intermediate chemical species shared among all the cases and the exclusive intermediates for each case are identified. Meanwhile, the intermediate species are quantified. Results show that the effects of the electric field on the reaction rates are not monotonic but highly nonlinear.

For the first time, mechanisms for the effects of an electric field with varying electric field strengths on the ethanol oxidation reactions are studied at the atomic scales. The reaction pathways without the electric field obtained by reactive molecular dynamics are consistent with previous studies, which validate the research methodology. The reaction pathways under varying electric field strengths show some common pathways but also unique pathways associated with individual electric field strengths. Such new insight into the mechanisms of reactions with an external electric field extends our understanding of assisted combustion, which may help to complete controllability theories [38] thereby developing control strategies for combustion. Finally, the present research demonstrates that ReaxFF-based reactive molecular dynamics is a valuable tool for detailed study of reaction mechanisms of hydrocarbon or oxygenated fuels, which complements commonly used experimental and computational techniques.

Acknowledgment

Funding from the UK Engineering and Physical Sciences Research Council under the projects “UK Consortium on Mesoscale Engineering Sciences (UKCOMES)” (Grants Nos. EP/L00030X/1 and EP/R029598/1) and “High Performance Computing Support for United Kingdom Consortium on Turbulent Reacting Flow (UKCTRF)” (Grant No. EP/K024876/1) is gratefully acknowledged. The first author gratefully acknowledges full support from the Dean’s Prize Scholarship of the Faculty of Engineering Sciences, University College London.

Supplementary materials

Supplementary material associated with this article can be found, in the online version, at doi:10.1016/j.proci.2018.07.053.

References

- [1] D. Bradley, S.M.A. Ibrahim, *Combust. Flame* 22 (1974) 43–52.
- [2] O. Imamura, B. Chen, S. Nishida, K. Yamashita, M. Tsue, M. Kono, *Proc. Combust. Inst.* 33 (2011) 2005–2011.
- [3] D. Bradley, S.H. Nasser, *Combust. Flame* 55 (1984) 53–58.
- [4] G.T. Kim, D.G. Park, M.S. Cha, J. Park, S.H. Chung, *Proc. Combust. Inst.* 36 (2017) 4175–4182.
- [5] Y.H. Gan, Z.B. Luo, Y.P. Cheng, J.L. Xu, *Appl Therm Eng* 87 (2015) 595–604.
- [6] F. Altendorfer, J. Kuhl, L. Zigan, A. Leipertz, *Proc. Combust. Inst.* 33 (2011) 3195–3201.
- [7] F.J. Weinberg, D. Dunn-Rankin, F.B. Carleton, S. Karnani, C. Markides, M. Zhai, *Proc. Combust. Inst.* 34 (2013) 3295–3301.
- [8] A.N. Hayhurst, J.M. Goodings, S.G. Taylor, *Combust. Flame* 161 (2014) 3249–3262.
- [9] G. Xiong, A. Kulkarni, Z.Z. Dong, S.Q. Li, S.D. Tse, *P Combust Inst* 36 (2017) 1065–1075.
- [10] Q. Bao, C. Pan, *Nanotechnology* 17 (2006) 1016–1021.
- [11] N. Leplat, P. Dagaut, C. Togbe, J. Vandooren, *Combust. Flame* 158 (2011) 705–725.
- [12] F. Rau, S. Hartl, S. Voss, M. Still, C. Hasse, D. Trimis, *Fuel* 140 (2015) 10–16.
- [13] K. Hirotsaka, M. Fukayama, K. Wakamatsu, Y. Ishida, K. Kitagawa, T. Hasegawa, *Proc. Combust. Inst.* 31 (2007) 3361–3367.
- [14] P. Saxena, F.A. Williams, *Proc. Combust. Inst.* 31 (2007) 1149–1156.
- [15] M. Aghsaei, D. Nativel, M. Bozkurt, M. Fikri, N. Chaumeix, C. Schulz, *Proc. Combust. Inst.* 35 (2015) 393–400.
- [16] Y. Luo, Y. Gan, X. Jiang, *Fuel* 188 (2017) 621–627.
- [17] O. Imamura, K. Yamashita, S. Nishida, G. Ianus, M. Tsue, M. Kono, *Combust. Sci. Technol.* 183 (2011) 755–763.
- [18] W. Somers, A. Bogaerts, A.C.T. van Duin, E.C. Neyts, *J. Phys. Chem. C* 116 (2012) 20958–20965.
- [19] K. Chenoweth, A.C.T. van Duin, W.A. Goddard, *Phys. Chem. A* 112 (2008) 1040–1053.
- [20] T.P. Senftle, S. Hong, M.M. Islam, et al., *Nat. Comput. Mater.* 2 (2016) 15011.
- [21] Q.D. Wang, J.B. Wang, J.Q. Li, N.X. Tan, X.Y. Li, *Combust. Flame* 158 (2011) 217–226.
- [22] J.E. Mueller, A.C.T. van Duin, W.A. Goddard, *J. Phys. Chem. C* 114 (2010) 5675–5685.
- [23] C. Ashraf, A.C.T. van Duin, *J. Phys. Chem. A* 121 (2017) 1051–1068.
- [24] A.C.T. van Duin, S. Dasgupta, F. Lorant, W.A. Goddard, *J. Phys. Chem. A* 105 (2001) 9396–9409.
- [25] M. Feng, X.Z. Jiang, K.H. Luo, *Proc. Combust. Inst.* (2018), doi:10.1016/j.proci.2018.05.109.
- [26] Q. Mao, Y. Ren, K.H. Luo, A.C.T. van Duin, *J. Chem. Phys.* 147 (2017) 244305.
- [27] Q. Mao, A.C.T. van Duin, K.H. Luo, *Carbon* 121 (2017) 380–388.
- [28] G. Xiao, K.H. Luo, X. Ma, S.J. Shuai, *Commun. Comput. Phys.* 4 (2018) 1241–1262.
- [29] S. Plimpton, *J. Comput. Phys.* 117 (1995) 1–19.
- [30] X.-M. Cheng, Q.-D. Wang, J.-Q. Li, J.-B. Wang, X.-Y. Li, *J. Phys. Chem. A* 116 (2012) 9811–9818.
- [31] M. Dontgen, M.D. Przybylski-Freund, L.C. Kroger, W.A. Kopp, A.E. Ismail, K. Leonhard, *J. Chem. Theory Comput.* 11 (2015) 2517–2524.
- [32] W. Humphrey, A. Dalke, K. Schulten, *J. Mol. Graph.* 14 (1996) 33–38.

- [33] G. Rotzoll, *J. Anal. Appl. Pyrolysis* 9 (1985) 43–52.
- [34] M. Aghsaei, D. Nativel, M. Bozkurt, M. Fikri, N. Chaumeix, C. Schulz, *Proc. Combust. Inst.* 35 (2015) 393–400.
- [35] L.R. Cancino, M. Fikri, A.A.M. Oliveira, C. Schulz, *Energy Fuels* 24 (2010) 2830–2840.
- [36] K. He, I.P. Androulakis, M.G. Ierapetritou, *Chem. Eng. Sci.* 65 (2010) 1173–1184.
- [37] T. Turányi, A.S. Tomlin, *Analysis of Kinetic Reaction Mechanisms*, Springer, 2016.
- [38] D.A. Drexler, J. Tóth, *J. Math. Chem.* 54 (2016) 1327–1350.